The Active GTP- and Ground GDP-Liganded States of Tubulin Are Distinguished by the Binding of Chiral Isomers of Ethyl 5-Amino-2-methyl-1,2-dihydro-3-phenylpyrido[3,4-*b*]pyrazin-7-yl Carbamate†

Pascale Barbier and Vincent Peyrot*

ESA-CNRS 6032, "Protéines et Cancer", Faculté de Pharmacie de Marseille, 27 boulevard Jean Moulin, F-13385 Marseille Cedex 5, France

Daniel Leynadier and José Manuel Andreu

Centro de Investigaciones Biologicas, Consejo Superior de Investigaciones Cientificas, Velazquez 144, 28006 Madrid, Spain

Received March 12, 1997; Revised Manuscript Received November 3, 1997⊗

ABSTRACT: NSC 613862 (*S*)-(−) and NSC 613863 (*R*)-(+) are the two chiral isomers of ethyl-5-amino-2-methyl-1,2-dihydro-3-phenylpyrido[3,4-*b*]pyrazin-7-yl carbamate. Both compounds bind to tubulin in a region that overlaps the colchicine site. They induce formation of abnormal polymers from purified GTP-Mg-tubulin, the active assembly form of tubulin, in glycerol-free buffer with magnesium [De Ines, C., Leynadier, D., Barasoain, I., Peyrot, V., Garcia, P., Briand, C., Rener, G. A., and Temple, C., Jr. (1994) *Cancer Res. 54,* 75−84]. In this study, we observed that the *S*-isomer can promote polymerization of GDP-tubulin, the inactive assembly-incompetent form of tubulin, into nonmicrotubular structures at a critical protein concentration of 1 mg/mL (12 mM $MgCl_2$). Neither the *R*-isomer nor colchicine have this ability. By electron microscopy, these tubulin polymers showed the same poorly defined filamentous structure when GDP-tubulin or GTP-Mg-tubulin were used. By HPLC measurements, we demonstrated that a dissociated GTP hydrolysis and exchange of nucleotide occurred during the isomer-induced abnormal assembly. Both isomers inhibited the Mg^{2+}-induced tubulin self-association leading to 42 S double ring formation from GTP-Mg-tubulin or GDP-tubulin. Measurement of their binding under nonassociation conditions revealed a 3-fold decrease in the apparent equilibrium binding constant of the *R*-isomer to GDP-tubulin relative to GTP-Mg-tubulin. For the *S*-isomer, the decrease in the binding constant was less pronounced. Binding data, analyzed in terms of a system of linked conformational and association equilibria, provide evidence that the active ("straight") rather than the inactive ("curved") conformation of tubulin differentially recognizes these ligands. Whereas binding of colchicine to tubulin is well-known to induce GTP hydrolysis, this is the first case in which the interaction of a ligand with the colchicine site is shown to be sensitive to the presence of GDP or GTP at the distant nucleotide binding site.

Tubulin is an $\alpha\beta$-heterodimer with two distinct nucleotide binding sites, an exchangeable (E-site) site and a functionally nonexchangeable site (N-site) (*1*). During microtubule assembly, GTP at the exchangeable site is hydrolyzed to GDP and orthophosphate (*2*, *3*). This process results in a GDP-tubulin wall and a GTP-tubulin cap stabilizing the microtubule (*4*−*7*). The stochastic loss and recovery of this cap generates the length fluctuations characteristic of microtubule dynamic instability (*8*). On the other hand, in presence of high concentrations of magnesium, the 5.8 S tubulin $\alpha\beta$-dimer is in rapid equilibrium with a 42 S species (*9*). This process, observed by sedimentation velocity, is best described in terms of a progressive isodesmic self-association of the tubulin dimer, characterized by an identical chain elongation equilibrium constant K_2, and terminated by a ring-closing step, at a degree of polymerization $n = 26 \pm 2$ (*10*, *11*). The ring-closing step entails an entropic contribution which is more favorable for GDP-tubulin than for GTP-Mg-tubulin (*12*). To explain the different stabilities of GTP-tubulin and GDP-tubulin microtubules, a model has been proposed (*12*, *13*) in which the tubulin dimer exists in an equilibrium between two states, a "straight" or microtubule-forming conformation and a "curved" or ring-forming conformation. The structure of tubulin double rings corresponds to pairs of microtubule protofilament segments curved tangentially to the microtubule surface (*14*). The equilibrium between the two forms is controlled by the nature of the nucleotide that occupies the exchangeable site (*13*). GTP favors the "straight" conformation, while GDP favors the "curved" conformation. The γ-phosphate of the guanine nucleotide in proper coordination with a magnesium ion determines the tubulin conformation (*15*, *16*). GDP- and GTP-tubulin in magnesium free solution have a ground state "curved"

† This work was supported by joint French-Spanish Grants: PICASSO (1995−1996), CSIC-CNRS agreement (1997), and DGICyT Grant PB 95-0116; D.L. held postdoctoral fellowships from MEC and the European Commission.

* To whom correspondence should be addressed. Tel: 33 4 91 83 56 16. Fax: 33 4 91 83 26 12.

⊗ Abstract published in *Advance ACS Abstracts,* December 15, 1997.

S0006-2960(97)00568-0 CCC: $15.00
Published on Web 01/13/1998

conformation, whereas GTP-Mg-tubulin has a "straight" conformation (*16*). Observation of microtubule ends by cryoelectron microscopy has shown structural differences during growing and shrinking phases. During growth, the microtubule ends form two-dimensional sheets closing into tubes, whereas during shrinkage the individual ends of protofilaments curl (*17*, *18*). To date, there is no other way to detect the "curved" and "straight" conformation than by their propagated assembly properties.

Other ligands besides nucleotides are able to induce tubulin conformational changes. The antimitotic compound colchicine induces a GTPase activity in tubulin (*2*) and alters the self-assembly behavior of tubulin (*19*, *20*). Under microtubule assembly conditions, the 1:1 tubulin−colchicine complex polymerizes into anomalous structures even in absence of glycerol (*19*, *20*). Like microtubule polymerization, this mechanism of self-assembly is characterized by a nucleated condensation process and a GTP hydrolysis. Moreover, the GDP-tubulin−colchicine complex remains inactive for assembly. Unlike microtubules, the hydrolysis of GTP occurred at the same intrinsic rate constant as in nonassociated protein, indicating a GTPase activity completely dissociated from the polymerization process (*19*, *21*). Colchicine has been extensively used to study *in vitro* tubulin self-association. On the other hand, numerous ligands bind to the colchicine site. Some of them are structural analogs, and others share only a partial hydrophobic character. These ligands can also be used to provide information about tubulin self-association processes. This is the case of two chiral isomers NSC 613862 (*S*)-(−) (CI980)[1] and NSC 613863 (*R*)-(+) (Chart 1). These molecules inhibit *in vitro* tubulin polymerization, bind with a high-affinity constant by overlapping the colchicine site, and induce a conformational change which promotes the formation of abnormal polymers and a GTPase activity in the tubulin dimer (*22*, *23*). These molecules also inhibit the polymerization of the cytoplasmic microtubules of PtK_2 cells and block these cells in metaphase, the *S*-isomer being more potent than the *R*-isomer (*23*). Fluorescence stopped-flow study of the interaction between the *R*- and *S*-isomers and tubulin has shown that the *R*-isomer binds in two steps: an initial binding followed by a conformational change of the initial complex (*24*). Related experiments done with the *S*-isomer showed that this compound has a slower kinetics of association than the *R*-isomer. Although this kinetic study did not explain the difference of activity between the two enantiomers, it demonstrated that the position of the methyl group influences the dissociation step. Note that only GTP-Mg-tubulin was employed in these previous studies.

This study aimed to gain information, first, on the origin of the difference in activity of the two enantiomers and, second, on the effects of tubulin conformational changes on their interactions. Indeed, ligand interactions with tubulin possibly linked with the E-site occupancy have been extensively pursued. The differing conformational changes induced by GTP-Mg or GDP at the E-site may affect ligand binding. We therefore examined the effects of *R*- and *S*-isomers in presence of high magnesium concentration on the self-assembly of tubulin (GTP-Mg- and GDP-) into abnormal polymers and into double rings. Comparing these results with those of the tubulin−colchicine interaction, we showed that the *R*- and *S*-isomers exhibit previously unknown effects. Only the *S*-isomer renders usually inactive GDP-tubulin competent to polymerize into abnormal filamentous structures. The two enantiomers inhibit the tubulin (GTP-Mg- and GDP-) self-association into double rings. In magnesium free buffer, their binding parameters show that these enantiomers distinguish between the two conformations of the tubulin dimer, the active GTP-Mg- and the ground GDP-liganded states.

Chart 1. Structures of the *R*- and *S*-Isomers

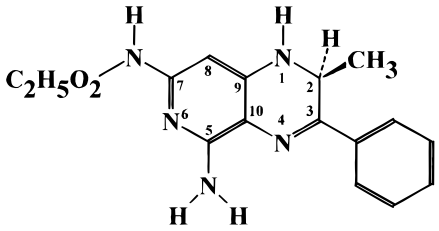

NSC 613862 (S) CI980

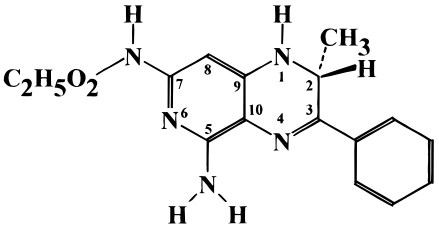

NSC 613863 (R)

MATERIALS AND METHODS

Protein and Chemicals. Tubulin was purified from calf brain by the modified procedure of Weisenberg (*25*−*27*), stored in liquid nitrogen and prepared for use as described below. Tubulin concentration was determined spectrophotometrically at 275 nm with an extinction coefficient of 1.09 L g^{-1} cm^{-1} in 6 M guanidine hydrochloride or 1.07 L g^{-1} cm^{-1} in 0.5% SDS in neutral aqueous buffer. The tubulin−colchicine complex was prepared as described, and its concentration was determined spectrophotometrically with an extinction coefficient of 1.14 L g^{-1} cm^{-1} in 1% SDS in neutral aqueous buffer (*20b*).

Colchicine (Aldrich Chemical Co.) concentration was spectrophotometrically measured employing an extinction coefficient $\epsilon_{350nm} = 16\,600\ M^{-1}\ cm^{-1}$. MTC was a gift from Dr. T. J. Fitzgerald (*27*); its concentration was determined spectrometrically with $\epsilon_{343nm} = 17\,600\ M^{-1}\ cm^{-1}$ (*27b*). NSC 613862 (CI980) (*S*) and NSC 613863 (*R*) were a gift from

[1] ABBREVIATIONS: NSC 613862 (*S*)-(−) (CI980) and NSC 613863 (*R*)-(+), ethyl 5-amino-2-methyl-1,2-dihydro-3-phenylpyrido-[3,4-*b*]pyrazin-7-yl carbamate; MTC, 2-methoxy-5-(2,3,4-trimethoxyphenyl)-2,4,6-cycloheptatrien-1-one; E-site, exchangeable nucleotide binding site; GTP: guanosine 5′-triphosphate; GDP, guanosine 5′-diphosphate; SDS, sodium dodecyl sulfate; Me_2SO, dimethyl sulfoxide; PG buffer, 10 mM sodium phosphate and 0.1 mM GTP, pH 7.0; EDTA, ethylenediaminetetraacetic acid; HPLC, high-performance liquid chromatography; PEDTA buffer, 10 mM phosphate, 1 mM EDTA, pH 7.0; $\Delta s_{20,w}$, difference sedimentation coefficient of liganded minus unliganded tubulin.

Dr. Renner (*28*). Stock solutions were made in Me_2SO and stored at −20 °C. Their concentrations were determined spectrophotometrically with extinction coefficients ϵ_{374nm} = 15 100 and 15 400 M^{-1} cm^{-1} for the *S* and *R* compounds, respectively (*28*). GTP (disodium salt) was from Fluka. GDP (sodium salt) was obtained from Pharmacia (lots AD1900103) and from Sigma (Type I, lot 54H7806). All other chemicals were of reagent grade.

Preparation of Tubulin with GTP in the Exchangeable Site (E-Site). Aliquots of protein were chromatographed in drained spin columns (1 × 5 cm) of Sephadex G25, equilibrated with PG buffer, followed by passage through a second larger (1 × 10 cm) gravity column of Sephadex G25 equilibrated with the same buffer. This standard tubulin preparation (*25*−*27*) consists of approximately 93% GTP liganded tubulin at site-E and contains residual Mg^{2+} (*29*), so we denominated this protein GTP-Mg-tubulin for the purpose of the present work.

Preparation of GDP-Tubulin. Tubulin with GDP occupying the exchangeable site was prepared by the two-step exchange procedure described by Diaz and Andreu (*29*). Protein samples were passed through a drained centrifuge column of Sephadex G25 medium (1 × 6 cm) equilibrated with 10 mM sodium phosphate buffer, 1 mM EDTA, and 1mM GDP, pH 7, in the cold. GDP (10 mM) was added to the protein, which was incubated on ice for 10 min. A second cold Sephadex G25 chromatography (1 × 10 cm) equilibrated with the same buffer was performed to remove the excess of nucleotide. HPLC analysis of the resulting protein showed that it contained 99% GDP at site E.

Binding Measurements by Fluorimetric Titration. Quenching of the intrinsic protein fluorescence as well as the increase in ligand fluorescence due to their interaction were employed to estimate the binding parameters of the *R*- and *S*-isomers to the different preparations of tubulin. GTP-Mg-tubulin and GDP-tubulin (3−7 μM) were titrated with various concentrations of *R*- and *S*-isomers and the bicyclic analog of colchicine, MTC. The fluorescence measurements were performed with a Perkin-Elmer Luminescence Spectrometer 50 with slit widths of 5/5 nm monitored by an IBM PS2 computer. Uncorrected fluorescence spectra were obtained by using 0.2 (excitation) × 1 cm cells (Hellma) thermostated at 25 °C by a circulating water bath. For protein quenching fluorescence titrations, emission fluorescence spectra (λ_{exc} = 295 nm) were collected, the fluorescence intensity values at 340 nm were corrected for the inner filter effect according to Lakowicz (*30*) and plotted versus *R* and *S* concentrations. The experimental curve was fitted as described by Barbier et al. (*31*) to determine the stoichiometry (*n*), the affinity constant (K_a), and the plateau fluorescence value (F_{max}). For the ligand fluorescence titrations, emission spectra (λ_{exc} = 380 nm) were collected. After correction for the inner filter effect, the fluorescence intensity values at 460 nm were plotted versus *R*-isomer concentrations, and the binding parameters fitted as described (*31*). The *R*-isomer also binds to GTP-Mg-tubulin at several lower affinity binding sites where the contribution to the fluorescence signal is negligible (*22*). To verify that its interaction with the lower affinity binding sites with GDP-tubulin is also negligible, we repeated titrations with the tubulin−colchicine complex. The emission fluorescence intensities of the GDP-tubulin−colchicine-ligand complex at 460 nm (λ_{exc} = 380 nm) were subtracted from those of the GDP-tubulin−ligand complex and analyzed as indicated above. Nonsignificantly different results were obtained.

Direct Binding Measurements. The Hummel-Dreyer (*32*) column gel permeation technique was used to measure the binding of the *R*-isomer to GTP-Mg-tubulin and GDP-tubulin. Bio-Gel P4 columns (0.9 × 12 cm) were equilibrated with 14 μM *R*-isomer in PG buffer for GTP-Mg-tubulin or in PEDTA and 1 mM GDP buffer for GDP-tubulin. A solution (0.7 mL) of 7−8 μM GDP or GTP-Mg-tubulin in the same buffer as that used for equilibration was applied to the column. The rest of the experimental procedure was as reported (*22*, *33*).

Formation of Abnormal Polymers. Ligand-induced assembly of tubulin into abnormal polymers was performed in PG buffer with 16 mM $MgCl_2$, pH 6.55, for GTP-Mg-tubulin, or in 10 mM sodium phosphate buffer, 12 mM $MgCl_2$, and 1 mM EDTA, 1 mM GDP, pH 6.60, for GDP-tubulin. The reaction was monitored turbidimetrically at 475 nm with a Beckman DU 7400 spectrophotometer. The protein samples (0.5−5 mg/mL) with saturating concentrations of *R*- and *S*-isomers were placed at 37 °C in spectrophotometer cells thermostated by a circulating water bath. The residual Me_2SO was less than 2%.

Electron Microscopy. Small aliquots of the assembly solution were adsorbed to carbon-coated Formvar films on copper grids, stained for 1 min in 2% uranyl acetate, and observed with a Philips EM 400 T electron microscope.

Measurement of Nucleotides during Tubulin Polymerization. Aliquots of the GTP-Mg-tubulin assembly solution with 10^{-4} M *R*- and *S*-isomers were removed at different times. Tubulin was precipitated by 0.5 M perchloric acid, centrifuged at 15 000 rpm for 10 min at 4 °C, and the nucleotide extracted from the supernatant (*34*). The nucleotides were quantified by tetrabutylammonium ion-pair HPLC (Supercosil LC-DB) with a known concentration of guanosine as an internal standard. The number of moles of nucleotide (GTP and GDP) per mole of tubulin in the reaction mixture was plotted versus time; the slopes represent the rough rate of GTP hydrolysis, which was taken as the mean of the rates of GTP disappearance and of GDP appearance. The net GTP hydrolysis rate value was calculated by subtracting the rate in the absence of ligand from that in the presence of ligand. In absence of ligand, the background GTP hydrolysis rate of the Weisenberg tubulin preparation was 0.0080 ± 0.0001 mol of GTP hydrolyzed (mol of tubulin)$^{-1}$ min^{-1} (dashed line in Figure 4C). This value was compatible with those found by Andreu and Timasheff (*35*) [0.0048 mol of GTP hydrolyzed (mol of tubulin)$^{-1}$ min^{-1}] and by Perez-Ramirez et al. (*36*) [0.013−0.015 mol of GTP hydrolyzed (mol of tubulin)$^{-1}$ min^{-1}] using a standard method with [γ-^{32}P]GTP.

To determine the nature of the nucleotide bound to tubulin in the polymer, we removed small aliquots of the assembly solutions at different times (from 3 to 130 min) and centrifuged them at 100 000 rpm (TLA 120.2 rotor) for 5 min at 37 °C in a Beckman Optima TLX ultracentrifuge. The pellets were washed with warm nucleotide-free buffer (10 mM sodium phosphate buffer at 37 °C), resuspended in this buffer, and then the nucleotides were extracted as described above. The supernatants were treated as described in the previous paragraph.

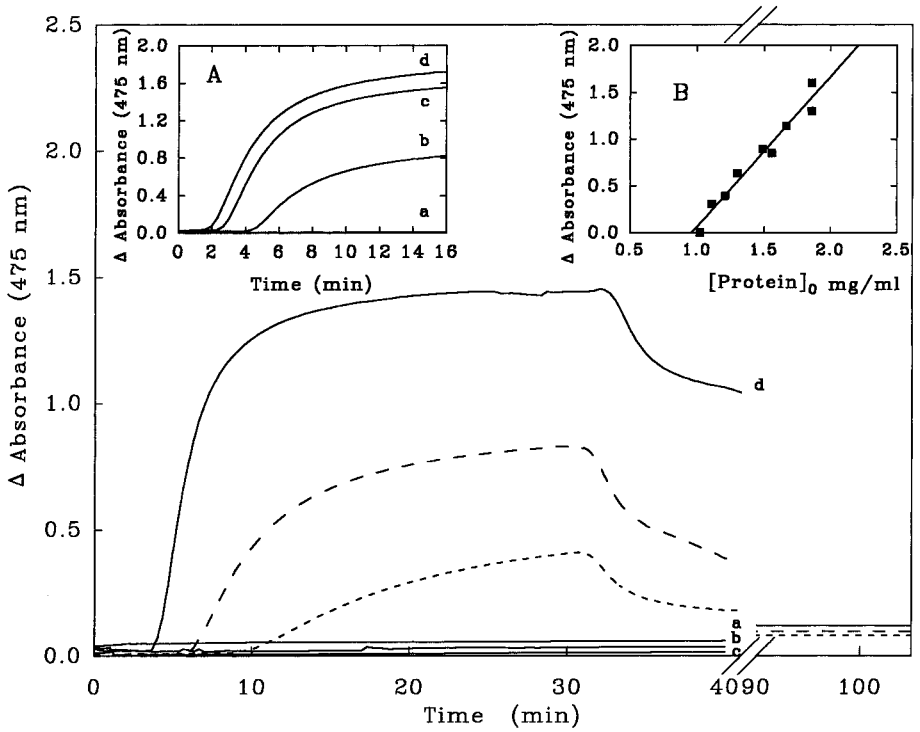

FIGURE 1: The solid lines are turbidimetrically monitored time courses of polymerization of GDP-tubulin (1.86 mg/mL) in PEDTA buffer, 1 mM GDP, and 12 mM $MgCl_2$ in presence of (a) no drugs, (b) 0.1 mM *R*-isomer, (c) 0.1 mM colchicine, (d) 0.1 mM *S*-isomer. The dashed lines represent the polymerization induced by *S*-isomer (0.1 mM) with 1.58 mg/mL (− −) and 1.21 mg/mL (- - -) tubulin. The reaction was started by warming the samples to 37 °C. After 30 min, the samples were cooled to 10 °C. At the times indicated by "//", the samples were placed in ice for 50 min. Inset A shows the magnesium concentration dependence of the abnormal polymers formation from 2.1 mg/mL tubulin with 0.1 mM *S*-isomer and 8 mM (a), 10 mM (b), 12 mM (c), and 14 mM (d) $MgCl_2$. Inset B shows the protein concentration dependence of the formation of abnormal polymers in presence of 0.1 mM *S*-isomer at 37 °C.

Sedimentation Velocity. All sedimentation velocity experiments were performed in a Beckman Model E analytical ultracentrifuge equipped with electronic speed control and RTIC temperature control. In the absence of Mg^{2+}, identical samples of GDP-tubulin (3−7 mg/mL) with and without ligand were run simultaneously in double-sector cells in a Beckman An-D rotor at 60 000 rpm at 20 °C.

The Mg^{2+}-induced self-association of GDP-tubulin or GDP-tubulin−colchicine complex was examined in 10 mM sodium phosphate buffer, 1mM EDTA, 1 mM GDP, and 12 mM $MgCl_2$, pH 6.60. GTP-Mg-tubulin or GTP-Mg-tubulin−colchicine complex were examined in 10 mM sodium phosphate buffer, 0.1 mM GTP, and 16 mM $MgCl_2$, pH 6.55. Under these conditions, bimodal sedimentation profiles were obtained. The two peaks reflect the sedimentation boundaries of a reversible associating system between tubulin dimers and rings (*10*−*12*). Identical samples of tubulin or tubulin−colchicine complex (6−14 mg/mL) with and without *R*- and *S*-isomers were run simultaneously in double-sector cells in a Beckman An-D rotor at 48 000 rpm at 20 °C. The bar angle was 60° in all measurements.

RESULTS

Effect of the Nucleotide Bound to Tubulin E-Site on the Formation of Abnormal Polymers Induced by the R- and S-Isomers. Both *R*- and *S*-isomers induced the polymerization of purified GTP-Mg-tubulin into abnormal polymers in glycerol-free buffer with 16 mM Mg^{2+} (*23*). This is a characteristic of the interaction of colchicine and its analogs with GTP-Mg-tubulin (see the introductory portion of this paper). It seemed of interest to study the effect of the presence of GDP bound the E-site of tubulin on the formation of these structures. We checked the effect of the *R*- and *S*-isomers and colchicine on GDP-tubulin. Figure 1 shows the turbidimetric time course of polymerization of GDP-tubulin in PEDTA buffer, 12 mM Mg^{2+} at 37 °C, with colchicine and the *R*- and *S*-isomers. GDP-tubulin is normally inactive for abnormal polymerization (trace a), but we observed an increase in the turbidity at 475 nm with 10^{-4} M *S*-isomer (trace d). Neither the *R*-isomer (trace b) nor colchicine (trace c) had this effect. For the *R*-isomer, no polymerization was observed even with 5 mg/mL tubulin at 42 °C (data not shown).

The assembly induced by the *S*-isomer was partially reversible by cooling the sample to 12 °C. A complete depolymerization was obtained after incubation of the samples during 50 min at 0−4 °C. Furthermore, addition of 1 mM GTP at the steady state of the GDP-tubulin assembly process followed by a decrease in the temperature to 12 °C induced a complete drop in turbidity (not shown). These observations indicate that the incomplete depolymerization observed at 12 °C (Figure 1) did not result from the presence of large irreversible tubulin aggregates, and that the polymers formed in the presence of GTP are more cold sensitive than those formed in the presence of GDP. As with GTP-Mg-tubulin, the formation of abnormal polymers induced by *S*-isomer with GDP-tubulin was characterized by a lag time, a magnesium concentration dependence (inset A of Figure 1). The critical concentration of GDP-tubulin was 1 mg/mL at 12 mM $MgCl_2$ (inset B of Figure 1), 2-fold higher than that obtained with GTP-Mg-tubulin (*23*). It remained practically unchanged even for a 2-fold lower

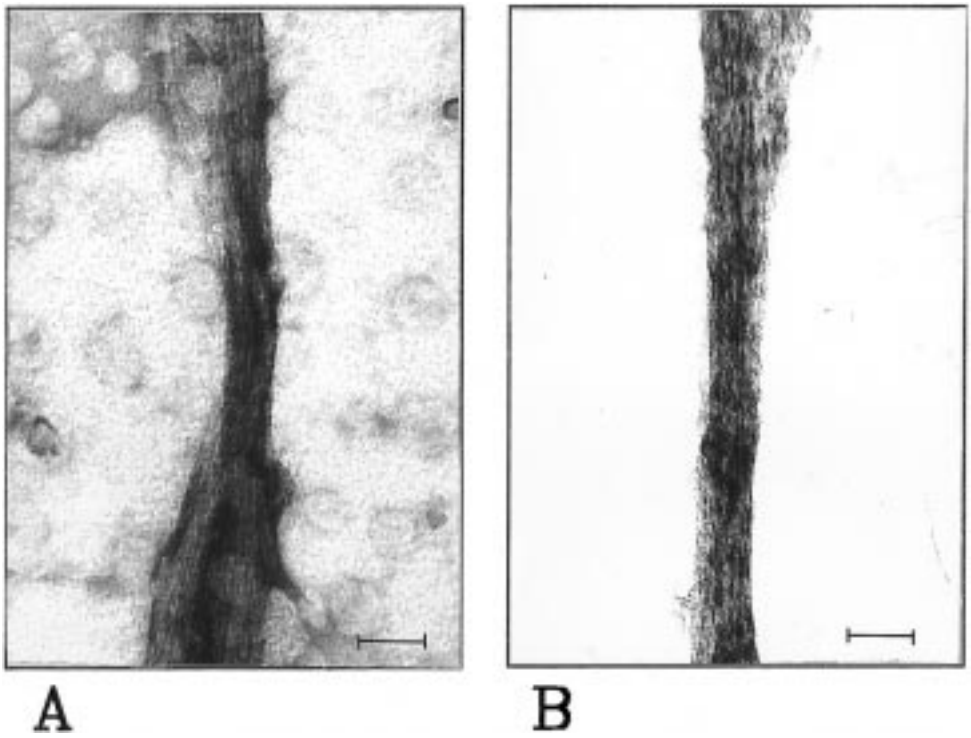

FIGURE 2: (A) Characteristic electron micrograph of abnormal polymers induced by the *S*-isomer from GTP-Mg-tubulin (PG buffer, 16 mM $MgCl_2$ at 37 °C). The bar represents 50 nm. (B) *S*-Isomer-induced abnormal polymers assembled from GDP-tubulin (PEDTA buffer, 1 mM GDP, and 12 mM $MgCl_2$ at 37 °C). The bar represents 71 nm.

concentration of *S*-isomer, suggesting that the *S*-isomer has a high affinity for the GDP-tubulin polymer.

Electron microscopy of the polymers formed from GTP-Mg-tubulin (Figure 2A) or GDP-tubulin (Figure 2B) with 10^{-4} M *S*-isomer showed poorly defined filamentous sheet structures in both cases, similar to the polymers formed from GTP-Mg-tubulin in presence of *R*-isomer (data not shown; see ref *23*). Thus, the *S*-isomer is the only colchicine-site ligand known to induce the assembly of GDP-tubulin. Faced with this observation, we then concentrated on the mechanism of formation of these structures and the role of nucleotides.

Formation of Abnormal Polymers and GTP Hydrolysis. In the presence of colchicine and with a low concentration of GTP, GTP-Mg-tubulin first polymerized into abnormal polymers and then depolymerized (Figure 3, trace b). This depolymerization was probably due to an accumulation of inactive GDP-tubulin, in agreement with the results of Saltarelli and Pantaloni (*19*). For the *R*- and *S*-isomers, however, no depolymerization was observed at 37 °C (Figure 3, traces c and d). At this stage, two hypotheses can be made: (1) there is no GTP hydrolysis during the formation of abnormal polymers induced by the *R*- and *S*-isomers and (2) the hydrolysis of GTP was slower for the *R*- and *S*-isomers than for colchicine. To distinguish between these hypotheses, we measured the nucleotide present in the solution during the formation of abnormal GTP-Mg-tubulin polymers in presence of *R*- and *S*-isomers (Figure 4, panels A and C). We observed an increase in GDP and a decrease in GTP concentrations, proving the presence of GTP hydrolysis. The net rates with the *R*- and *S*-isomers were 0.0028 ± 0.0007 and 0.0092 ± 0.0003 mol of GTP hydrolyzed (mol of tubulin)$^{-1}$ min^{-1}, respectively (see Materials and Methods), slower than that of colchicine [0.016

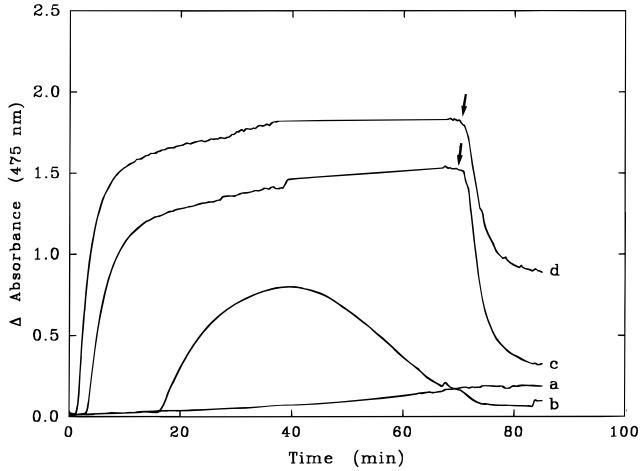

FIGURE 3: Polymerization of tubulin in 10 mM sodium phosphate buffer, 20 μM GTP, 16 mM $MgCl_2$ at 37 °C, induced by no drug (trace a), 35 μM colchicine (trace b), 35 μM *R*-isomer (trace c) and 35 μM *S*-isomer (trace d). The protein concentration was 2 mg/mL. At the time indicated by the arrow, the samples were cooled to 10 °C.

mol of GTP hydrolyzed (mol of tubulin)$^{-1}$ min^{-1} (*21*)]. This offered an explanation for the lack of depolymerization observed with the isomers (Figure 3, curves c and d), since there is a substantial amount GTP which has not yet been hydrolyzed. In the case of *S*-isomer, some polymers with GDP-tubulin must be formed, accounting for the difference in intensity of the cold-induced depolymerization for the *R*- and *S*-isomers.

To further characterize the mechanism of formation of abnormal polymers induced by the *R*- and *S*-isomers, we separately determined the amounts of GTP and GDP in the polymers (Figure 4, panels B and D) and in the solvent as described in Materials and Methods. GTP and GDP in the

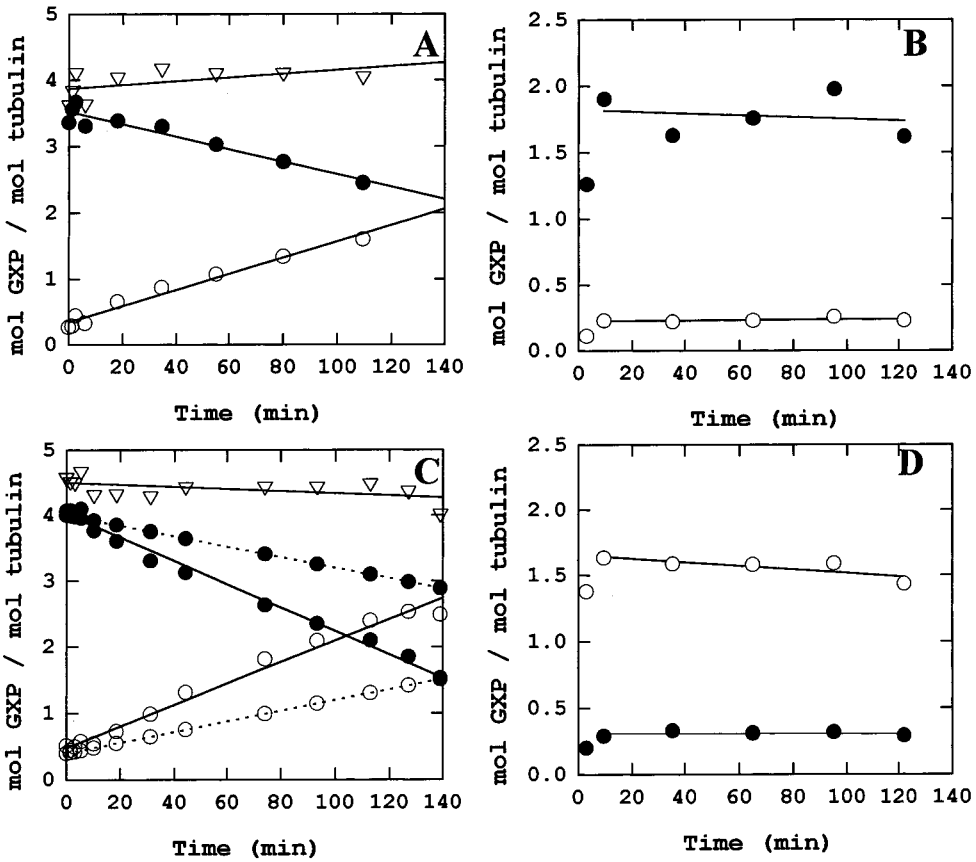

FIGURE 4: HPLC quantification of the amount of GTP and GDP during the formation of abnormal polymers induced by 0.1 mM *R*-isomer (A, B) and *S*-isomer (C, D) in PG buffer, 16 mM $MgCl_2$ at 37 °C. During the polymerization process, aliquots of GTP-Mg-tubulin (15 μM) were removed at different times and centrifuged to separate the polymers from the medium. Left panels represent the time course of variation of GTP (●) and GDP (○) found in the total reaction medium, ▽ represents the sum of GTP and GDP. Dashed lines in panel C represent the time course of nucleotide variation in absence of ligands. Right panels show GTP (●) and GDP (○) time course in the polymers (pellet) with 0.1 mM *R*- (B) or *S*- (D) isomer.

supernatant (not shown) varied linearly with time, similarly to the previous experiment (Figure 4, panels A and C). This linear time dependence of the amounts of GDP and GTP, as well as the independence with tubulin concentration (data not shown), demonstrated that the GTP hydrolysis was not linked with the formation of abnormal polymers induced by 10^{-4} M *R*- and *S*-isomers, which is a highly cooperative phenomenon characterized by a sigmoidal time course and the presence of a critical tubulin concentration. When the steady state was reached (about 10 min), the amounts of GTP and GDP in the pellet remained constant (Figure 4, panels B and D). This observation indicated that the GTP site was accessible in the polymer as well as in the soluble dimer. In summary, GTP hydrolysis and an exchange of nucleotide take place during the abnormal assembly induced by *R*- and *S*-isomers, which are dissociated from the polymerization process.

Effect of R- and S-Isomers on the Tubulin Self-Association Induced by Mg^{2+}. Tubulin can undergo Mg^{2+}- induced self-association leading to typical structures other than bidimensional microtubule-like polymers; these are the 42 S double rings (see the introductory portion of this paper). Colchicine very slightly enhances the strength of the intertubulin bonds in the self-association of tubulin dimers into rings (*15*). Since the *R*- and *S*-isomers bind overlapping the colchicine site, we concentrated our attention on the effects of the two enantiomers on this second mode of tubulin self-association. Above a given concentration of tubulin and magnesium, the sedimentation pattern of GTP-Mg-tubulin (Figure 5A) and GDP-tubulin (Figure 5D) became bimodal, the region between the peaks never reaching the base line, which is characteristic of a Gilbert self-association system (*37*). This bimodal sedimentation profile is an indication of formation of larger size species, the double rings (note, however, that the two peaks as such are not tubulin dimers and rings, but sedimentation boundaries of this reversible associating system). As expected, GDP-tubulin had a much stronger propensity (hypersharp appearance of the fast moving boundary) to form double rings than did GTP-Mg-tubulin (Figure 5, panels A and D). In presence of *R*-isomer, the area under the rapid peak decreased and the area under the slow peak increased. This is most simply interpreted as an inhibition of the tubulin association leading to ring formation, both for GTP-Mg-tubulin (Figure 5A) and GDP-tubulin (Figure 5D). In similar experiments with the *S*-isomer, the bimodal sedimentation profile disappears with GTP-Mg-tubulin (Figure 5B) and the area under the rapid peak largely decreases with GDP-tubulin (Figure 5E). Note that the accompanying decrease in the area of the slow peak in Figure 5B is also consistent with large polymers being pelleted out. In fact, in the presence of *S*-isomer at 20 °C, GTP-Mg-tubulin was able to form abnormal polymers with a critical concentration of about 4 mg/mL. In conclusion, the *S*-isomer was a more potent inhibitor of ring formation than the *R*-isomer irrespective of the GDP or GTP nucleotide bound to the E-site.

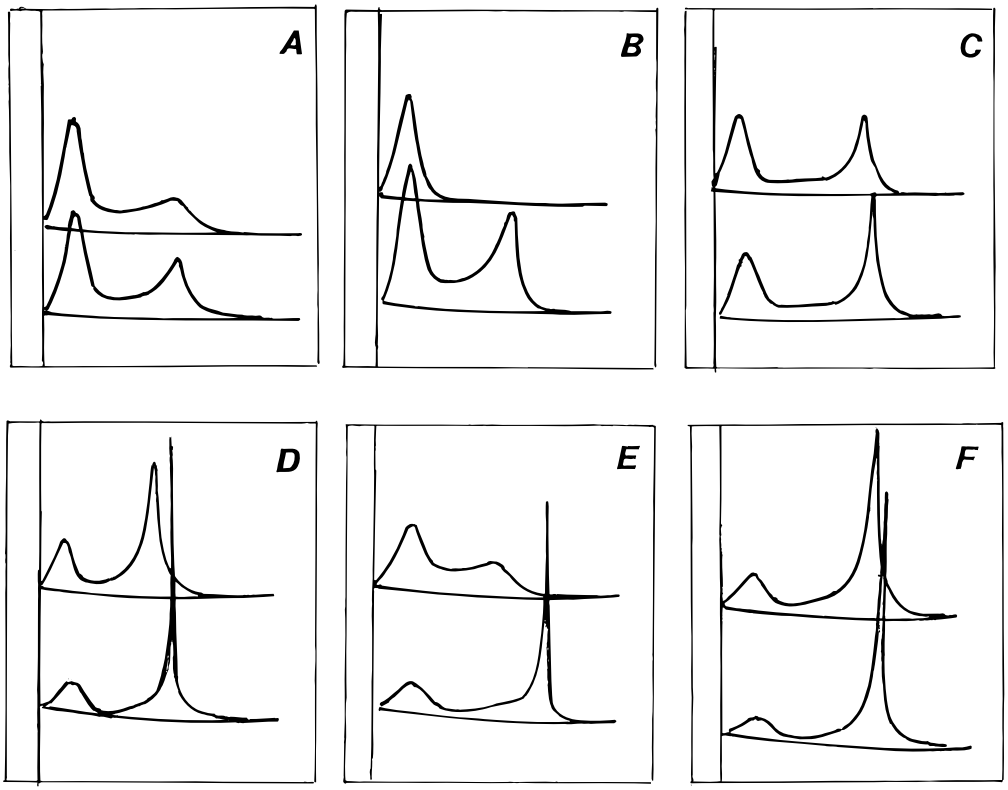

FIGURE 5: Effects of the presence of the *R*- and *S*-isomer on the tubulin self-association leading to double ring formation. Sedimentation velocity profiles of (A) GTP-Mg-tubulin (12.5 mg/mL) in PG buffer, 16 mM $MgCl_2$, in presence (upper) or in absence (lower) of 0.1 mM *R*-isomer, (B) GTP-Mg-tubulin (13.5 mg/mL) in the same conditions in presence (upper) or in absence (lower) of 0.1 mM *S*-isomer. The photograph was taken 12 min after reaching speed. Sedimentation velocity profiles (D) of GDP-tubulin (7.8 mg/mL) in PEDTA buffer containing 12 mM $MgCl_2$ and 1 mM GDP, in presence (upper) or in absence (lower) of 0.1 mM *R*-isomer. The photograph was taken 8 min after reaching speed. Sedimentation velocity profiles (E) of GDP-tubulin (7.5 mg/mL) in the buffer described above in presence (upper) or in absence (lower) of 0.1 mM *S*-isomer. The photograph was taken 16 min after reaching speed. Sedimentation velocity profiles of (C) GTP-Mg-tubulin−colchicine (14 mg/mL) and (F) GDP-tubulin−colchicine (7 mg/mL) complexes in presence (upper) and in absence (lower) of 0.1 mM *S*-isomer. The photographs were taken 12 min after reaching speed. Runs were performed at 48 000 rpm at 20 °C; sedimentation was left to right.

The *R*- and *S*-isomers bind to tubulin at one high-affinity site (colchicine site) and to several low-affinity sites (*22*). To verify that the inhibition of ring formation did not result from enantiomer binding to this second class of sites, we investigated the effect of both isomers on ring formation with the tubulin−colchicine complex. Neither the *R*-isomer nor the *S*-isomer were able to significantly inhibit the ring formation from GTP-Mg-tubulin−colchicine (Figure 5C) and GDP-tubulin−colchicine (Figure 5F) complexes. This result indicates that the inhibition of ring formation by both isomers is due to binding to the high-affinity site.

Binding of R- and S-Enantiomers to GTP-Mg- and GDP-Tubulin in Mg^{2+} Free Buffer. The results above show that the behavior of the two isomers differs with the nucleotide used. We wondered whether the affinity of these isomers for the different conformations of the tubulin heterodimer would also differ. It was necessary to establish whether the binding reaction is independent of protein−protein interactions. In magnesium free buffer, the *R*- and *S*-isomers induced no self-association of GTP-Mg-tubulin (*22*). We verified the association state of GDP-tubulin in the presence of those compounds by comparative sedimentation velocity measurements. The sedimentation velocity profiles of GDP-tubulin in the presence of *R*- and *S*-isomers consisted of a single symmetrical peak with $s_{20,w} = 5$ S at 5 mg/mL tubulin (not shown). Moreover, the increments $\Delta s_{20,w}$ in the presence of these ligands (10^{-4} M) were only 0.05 and 0.07 S for *R*- and *S*-isomers, respectively. These results demonstrated that neither isomer induced significant self-association of the GDP-tubulin heterodimer, therefore, permitting the measurement of their intrinsic binding under identical solution conditions.

Binding of the *R*- and *S*-isomers quenches the tryptophan tubulin fluorescence and increases the ligand fluorescence by energy transfer. These two properties were used to determine their apparent equilibrium constants of binding to GTP-Mg- and GDP-tubulin (Materials and Methods). The quenching of the intrinsic protein signal by the *R*-isomer (Figure 6A) indicated a marked decrease in the affinity for GDP-tubulin relative to GTP-Mg-tubulin. This was less pronounced for the *S*-isomer (Figure 6B). To compare these effects, the apparent association constants of the two isomers for both tubulin preparations are summarized in Table 1 as K_a ratios. The *S*-isomer showed a 1−2-fold decrease in its apparent affinity constant for GDP-tubulin relative to GTP-Mg-tubulin. More interestingly, the *R*-isomer had a 3−4-fold decrease (Table 1). When 1 mM GTP and 2 mM $MgCl_2$ were added to GDP-tubulin in the 1 mM EDTA-containing buffer, to back-exchange GTP in the E-site (*30*), an apparent affinity constant similar to that found for GTP-Mg-tubulin was obtained for the *R*-isomer (Table 1). This confirmed that the variation in the affinity of the *R*-isomer was linked with the nature of the nucleotide in the E-site. Addition of 1 mM GTP to GDP-tubulin without Mg^{2+} (a control without

Table 1: Comparison of MTC, *R*- and *S*-Isomer Binding to GDP- and GTP-Mg-Tubulin at 25 °C

procedure	ligand	parameter	$K_a \times 10^{6}$ [a] (M^{-1})	ratio[b]
quenching	R	K_a (GDP)	0.29 ± 0.05	
		K_a (GTP)	1.13 ± 0.57	
		K_a (GTP)/K_a (GDP)		4.0 ± 2.7
		K_a (GTP)/K_a (GDP → GTP)		1.0 ± 0.7
		.K_a (GTP)/K_a (GDP) + GTP		3.0 ± 1.2
	S	K_a (GDP)	1.51 ± 0.64	
		K_a (GTP)	2.53 ± 0.66	
		K_a (GTP)/K_a (GDP)		1.7 ± 1.2
		K_a (GTP)/K_a (GDP) + GTP		1.7 ± 0.9
	MTC	K_a (GDP)	0.31 ± 0.07	
		K_a (GTP)	0.32 ± 0.06	
		K_a (GTP)/K_a (GDP)		1.0 ± 0.4
ligand fluorescence	R	K_a (GDP)	1.67 ± 0.42	
		K_a (GTP)	5.00 ± 0.13	
		K_a (GTP)/K_a (GDP)		2.6 ± 0.7
		K_a (GTP)/K_a (GDP → GTP)		1.0 ± 0.4

[a] Average value of three independent determinations. [b] Average value of the ratios of three independent determinations in which both samples were titrated in parallel.

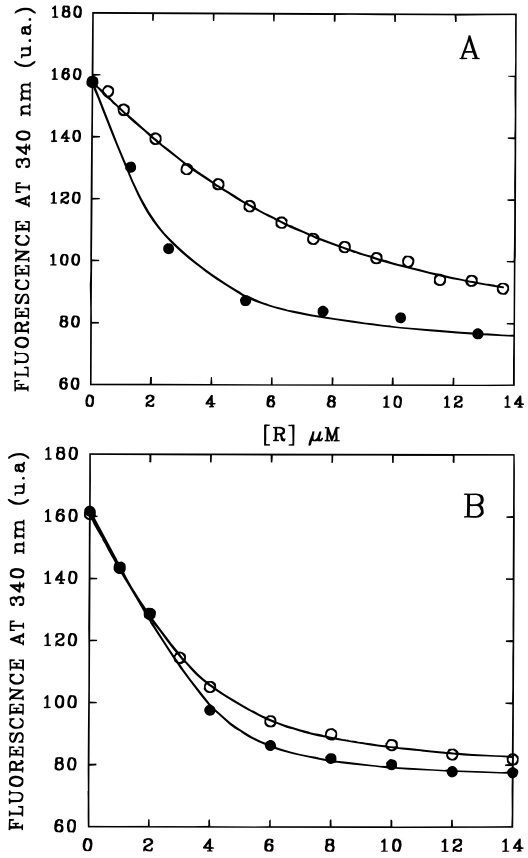

FIGURE 6: Representative protein fluorescence quenching titration curves of the interaction of *R*-isomer (A) and *S*-isomer (B) with (5 μM) GTP-Mg-tubulin (●) and GDP-tubulin (○) at 25 °C. The points represent experimental data and solid lines the fitted curves (see Materials and Methods). For the *R*-isomer, K_a values were (1.23 ± 0.18) × 10^6 M^{-1} (n = 0.93 ± 0.04 and F_{max} = 70.30 ± 0.70) and (3.43 ± 1.73) × 10^5 M^{-1} (n = 1.00 ± 0.16 and F_{max} = 69.69 ± 6.13) for GTP-Mg-tubulin, and GDP-tubulin respectively. For the *S*-isomer, K_a values were (3.05 ± 0.84) × 10^6 M^{-1} (n = 0.88 ± 0.04 and F_{max} = 75.06 ± 0.72) and (1.23 ± 0.21) × 10^6 M^{-1} (n = 0.94 ± 0.05 and F_{max} = 74.86 ± 1.19) for GTP-Mg-tubulin and GDP-tubulin, respectively.

back-exchange) did not modify the binding constants (Table 1).

Since the apparent affinity constant of *R*-isomer was the more nucleotide sensitive, we did similar experiments employing the increase in the ligand fluorescence promoted by the formation of the complex. As in protein quenching titration experiments, we observed a decrease in the *R*-isomer affinity for GDP-tubulin relative to GTP-Mg-tubulin (ratio = 2.6). After nucleotide back-exchange (GDP → GTP), the ratio reached 1, confirming again that the variation in *R*-isomer binding was related to the nucleotide in the E-site.

The *R*- and *S*-isomers also bind to several other lower affinity sites (*22*). To verify if the difference in the apparent binding constants results from their binding to the high affinity site (the colchicine site), we investigated the binding of the *R*-isomer to the tubulin−colchicine complex. The titration of GDP-tubulin−colchicine with various concentrations of *R*-isomer gave the same fluorescence emission values as with GTP-Mg-tubulin−colchicine (data not shown). This indicated a nucleotide-independent behavior of the lower affinity binding sites and proved the involvement of the high-affinity binding site in the differences observed (Table 1).

The direct gel chromatography procedure of Hummel and Dreyer (*32*) was also employed to examine the equilibrium binding of the *R*-isomer to GTP-Mg- and GDP-tubulin. This technique allows the measurement of the bound and free ligand. For a subsaturating concentration of *R*-isomer (14 μM, free concentration), this interaction was characterized by a binding ([*R*-isomer bound]/[protein]) of 0.945 ± 0.014 and 0.869 ± 0.015 for GTP-Mg-tubulin (8.85 μM) and GDP-tubulin (7.63 μM), respectively. These values confirm that the stoichiometry is unitary, that is, the weaker binding of the *R*-isomer to GDP-tubulin observed with the fluorescence methods is due to a reduction of the binding affinity. In fact, these single-point binding data were compatible with equilibrium constants yielding a ratio of 3 [$K_{a(GDP)}$ = 0.5 × 10^6 M^{-1} and $K_{a(GTP)}$ = 1.2 × 10^6 M^{-1}], similar to the fluorescence measurements.

Finally, to compare the behavior of both enantiomers with that of colchicine and its analogues, we determined the affinity of binding of the bicyclic analogue of colchicine MTC to GTP-Mg- and GDP-tubulin. This compound had the same affinity constant for the two tubulin preparations (ratio = 1, see Table 1). The difference in the binding constant depending on the nucleotide and cation found in the E-site of tubulin seems to be a characteristic of the *R*-

Scheme 1

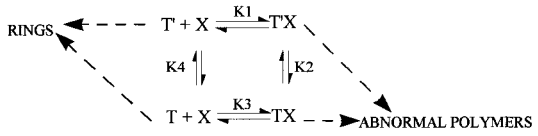

and *S*-interactions with tubulin, which behave differently from the colchicine structural analogue MTC.

DISCUSSION

Preferential Binding of the R- and S-Isomers to the Active Conformation of Tubulin. The *R*- and *S*-isomers bind to tubulin on the β-subunit, overlapping with colchicine binding. However, the colchicine site is more than 24 Å from the E-GXP-site (*38*). Any difference in the recognition of the *R*- and *S*-isomers by tubulin liganded to GTP or GDP in Mg^{2+}-free buffer must be due to an allosteric effect. We propose the following as the simplest scheme in which conformation and ligand binding equilibria are linked to explain such differences.

In Scheme 1, T and T′ are two different conformations of the protein, and X represents the ligand. The dashed lines are shown only to indicate the self-association behavior of the system with added magnesium, to be discussed later. In this scheme, there are two pathways leading to the same TX complex, which implies $K_1K_2 = K_3K_4$. The apparent binding affinity constant is $K_{app} = [TX]+[T'X]/([T]+[T'])[X]$. It can be expressed as a function of the microscopic constants, $K_{app} = K_1 + K_4K_3/(1 + K_4)$. Therefore, the apparent binding which is measured may be substantially different from the intrinsic binding, because of the displacement of the conformational equilibrium. For such linkage effect to occur, K_1 must be different from K_3. By model definition, K_1 and K_3 are intrinsic affinity constants of ligand binding to the two forms of tubulin T and T′. These constants are characteristic of the ligand and nucleotide independent. Thus, $K_{1(GTP)} = K_{1(GDP)} = K_1$ and $K_{3(GTP)} = K_{3(GDP)} = K_3$. By contrast, $K_{2(GTP)} \neq K_{2(GDP)}$ and $K_{4(GTP)} \neq K_{4(GDP)}$. For each isomer, we determined the value of K_{app} for GTP-Mg-tubulin and for GDP-tubulin. It holds that

$$K^{T}_{app} = 1 + K_{4T}(K_3/K_1)/1 + K_{4T} \quad (1)$$

$$K^{D}_{app} = 1 + K_{4D}(K_3/K_1)/1 + K_{4D} \quad (2)$$

$$K^{T}_{app}/K^{D}_{app} = (1 + K_{4T}\,(K_3/K_1)\,(1 + K_{4D}))/(1 + K_{4D}(K_3/K_1)\,(1 + K_{4T})) \quad (3)$$

where T and D stand for GTP and GDP, respectively. In the case of a positive linkage, $K_3 > K_1$ and $K_3/K_1 > 1$. Then $K^{T}_{app}/K^{D}_{app} > 1$ implies that $K_{4T}(K_3 - K_1) > K_{4D}\,(K_3 - K_1)$. Since $K_3 - K_1 > 0$, $K_{4T} > K_{4D}$. Since $K_1K_2 = K_3K_4$, at constant K_1K_3, $K_{4T} > K_{4D}$ implies that $K_{2T} > K_{2D}$. For both isomers, but mainly for the *R*-isomer, we observed a lower apparent affinity constant for GDP-tubulin than for GTP-Mg-tubulin. As described above, this implies that $K_{2T} > K_{2D}$ and $K_{4T} > K_{4D}$. The severalfold larger effective affinity of the apparent binding of *R*-isomer to GTP-Mg-tubulin than to GDP-tubulin indicates that the intrinsic conformational equilibrium constant of formation of the more actively binding species is severalfold larger for GTP-Mg-tubulin than for GDP-tubulin. We propose that T and T′ are, respectively, the "straight" active conformation of tubulin and the "curved" inactive conformation described by Shearwin et al. (*16*). In the presence of a high concentration of magnesium, T assembles into microtubules or abnormal polymers, whereas T′ associates to form double rings.

The value of the binding constants of the *R*- and *S*-isomers in this work (Figure 6 and Table 1) was slightly different from those determined by Leynadier et al. (*22*). This discrepancy can probably be attributed to the different methods of inner filter effect correction and of affinity constant analysis employed. However, this does not affect the purpose of the present measurements, which is to compare GTP-Mg-tubulin with GDP-tubulin, and *R*- with *S*-isomers.

The nucleotide back-exchange raises the binding affinity constant of the *R*-isomer back to that of GTP-Mg-tubulin. This increase indicates that a magnesium ion in proper coordination with the γ-phosphate of the E-guanine nucleotide site is required to produce the conformational switch of tubulin from the inactive ground state to active form (*16*).

Comparative experiments done with the bicyclic analog of colchicine, MTC, showed that identical binding constants were obtained for GTP-Mg- and GDP-tubulin, demonstrating that the tubulin conformational change does not affect the interaction of MTC. To our knowledge, the *R*-isomer and, less so, the *S*-isomer are the first probes known to distinguish between the two conformations of the tubulin heterodimer.

Inhibition by the R- and S-Isomers of the Mg^{2+}-Induced Tubulin Self-Association Leading to Double Ring Formation. Tubulin is able to associate into different structures, including microtubules (*39*, *40*), double rings (*10*, *11*), sheets, spiral ribbons, and abnormal filamentous polymers. While the last three structures require the binding of exogenous ligands such as Zn^{2+}, vinca alkaloids, or colchicine, respectively, the first two require Mg^{2+} ions. Actually, microtubules and rings are formed under similar solution conditions (*40*). In fact, the structure of the final polymer is controlled by the strong binding of one magnesium ion to GTP-tubulin in the "straight" conformation, which displaces the equilibrium from the ring-forming state to the microtubule-forming conformation (*16*). We have demonstrated that the *R*- and *S*-isomers inhibit ring formation. This could be directly linked, on the one hand, with an inhibition of the closing step, and/or on the other hand, with a decrease in the value of the equilibrium constant of the Mg^{2+}-induced isodesmic self-association process. An in depth understanding of the linkages involved in the inhibition of ring formation from GTP-Mg- and GDP-tubulin by the *R*- and *S*-isomers and the confirmation of the stronger effect for the *S*-isomer will require quantitative studies of the linkage between the binding of the two isomers and the tubulin association processes. However, the inhibition effect supports the conclusion that the *R*- and *S*-isomers bind preferentially to the active conformation of tubulin induced by GTP-Mg binding.

Induction of Abnormal Polymerization of GDP-Tubulin by the S-Isomer. Only the *S*-isomer induced the formation of abnormal polymers from the 1:1 GDP-tubulin complex. Comparison of the abnormal polymerization of GTP-Mg- and GDP-tubulin in presence of this isomer indicates that

(1) the polymers formed with GDP-tubulin are more cold-stable than those formed with GTP-Mg-tubulin and (2) the poorly defined filamentous polymers are similar with GDP or GTP at the E-site. For the *S*-isomer, the variation in free energy change resulting from abnormal polymer growth was favorable to GTP ($\Delta\Delta G_{appGTP-GDP} = -1.7$ kJmol^{-1} K^{-1}). For the *R*-isomer, this difference in free energy change is larger, and it is impossible to calculate because of the absence of observable polymer formation from GDP-tubulin. This is consistent with the *S*-isomer being a more powerful inhibitor of ring formation from GDP-tubulin than the *R*-isomer.

Some other ligands are able to induce the self-assembly of GDP-tubulin. Paclitaxel and its semisynthetic side chain analog docetaxel induce assembly of inactive GDP-tubulin into microtubules (*29*). In the presence of zinc ions, protofilaments form and aggregate into antiparallel sheets even with GDP at the E-site (*41*). The formation of microtubules or colchicine-induced abnormal polymers needs GTP-Mg-tubulin, and GTP hydrolysis leads to GDP-tubulin, which is unable to polymerize again. As in paclitaxel-induced microtubules and Zn-induced sheet formation, in the *S*-isomer−tubulin complex, the formation of abnormal polymers is not linked with GTP hydrolysis (see below), and GDP-tubulin is rendered active.

GTP Hydrolysis Is Dissociated from Tubulin Polymerization Induced by Both Isomers. The tubulin−colchicine complex can polymerize into nonmicrotubular polymers; this mechanism of polymerization has been studied in detail (*19*, *21*). It proceeds as a nucleated condensation polymerization which requires Mg^{2+}. A GTPase activity proceeds unlinked with polymerization, i.e., the soluble tubulin−colchicine complex and the abnormal tubulin−colchicine polymers hydrolyze the GTP at the same rate. These characteristics were also found for the *R*- and *S*-isomer−tubulin complexes. Indeed, if we relate the GTPase activity during the tubulin self-assembly in presence of *R*- and *S*-isomers to the GTPase activity of tubulin−colchicine (100%) (*21*), we obtain 56% for the *S*-isomer and 18% for the *R*-isomer. These values agree with those previously found (*22*) under nonassembly conditions with the standard radioactive method ([γ-^{32}P]-GTP). This confirms that the GTPase activity induced by both enantiomers was not linked with the polymerization process.

In conclusion, the binding of the *R*- and *S*-isomers to the GTP-Mg-tubulin produced a protein conformational change which induced a GTPase activity and the formation of abnormal polymers (*22*). This conformational change was different from that produced by colchicine because, whereas this ligand slightly increases ring formation, the two enantiomers inhibit it. Moreover, although the equilibrium constant of the interaction of the bifunctional analog of colchicine (MTC) with GTP-Mg- and GDP-tubulin remained unchanged, we observed a slight decrease and a 3-fold decrease for the *S*- and *R*-isomer, respectively. This observation also accounts for the different behaviors of the enantiomers relative to colchicine. The Raman bands of the *R*-isomer due to the stretching of C═C from the phenyl ring are strongly modified during its interaction with tubulin (*42*). Moreover, the *R*-isomer developed the strongest increase in fluorescence intensity upon binding to tubulin and has the strongest value of the dihedral angle between the phenyl group and the pyridopyrazine ring (*31*). These two observations have been interpreted as revealing a different localization of the two isomers in the binding site, the *R*-isomer being more anchored in the binding locus. This agrees with the stronger influence of the tubulin conformation on the binding affinity of the *R*-isomer. This important result indicates that both isomers, and especially the *R*-isomer, are able to distinguish between the active "straight" and the inactive "curved" conformation of $\alpha\beta$-tubulin dimer, providing a molecular probe for recognition of the two tubulin conformations. Also, it is important to note that the *S*-isomer has an original behavior; indeed, we show that a colchicine-site ligand can induce the polymerization of GDP-tubulin into filamentous structures. This characteristic was reserved to the taxoids, which induce GDP-tubulin polymerization into microtubules (*29*). It appears that the mechanisms of action of both enantiomers differ from those of colchicine and paclitaxel.

ACKNOWLEDGMENT

We thank H. Bouteille for analytical ultracentrifugation experiments, Dr G. A. Renner for the gift of *R*- and *S*-isomers, and Dr T. J. Fitzgerald for the gift of MTC.

REFERENCES

1. Jacobs, M., Smith, M., and Taylor, K. W. (1974) *J. Mol. Biol.* 89, 455−468.
2. David-Pfeuty, T., Erickson, H. P., and Pantaloni, D (1978) *Proc. Natl. Acad. Sci. U.S.A.* 74, 5372−5376.
3. MacNeal, R. K., and Purich, D. L. (1978) *J. Biol. Chem.* 253, 4683−4687.
4. Carlier, M. F., and Pantaloni, D. (1981) *Biochemistry* 20, 1918−1924.
5. Mitchison, T., and Kirchner, K. (1984) *Nature* 312, 232−237.
6. Mitchison, T., and Kirchner, K. (1984) *Nature* 312, 237−242.
7. Carlier, M. F. (1991) *Curr. Opin. Cell Biol.* 3, 12−17.
8. Bayley, P., Schilstra, M. J., and Martin, S. (1990) *J. Cell Sci.* 95, 33−48.
9. Weisenberg, R. C., and Timasheff, S. N. (1970) *Biochemistry* 9, 4110−4116.
10. Frigon, R. P., and Timasheff, S. N. (1975) *Biochemistry* 14, 4559−4566.
11. Frigon R. P., and Timasheff, S. N. (1975) *Biochemistry* 14, 4567−4573.
12. Howard, W. D., and Timasheff, S. N. (1986) *Biochemistry* 25, 8292−8300.
13. Melki, R., Carlier, M. F., Pantaloni, D., and Timasheff, S. N. (1989) *Biochemistry* 29, 8921−8932.
14. Diaz, J. F., Pantos, E., Bordas, J., and Andreu, J. M. (1994) *J. Mol. Biol.* 238, 214−225.
15. Shearwin, K. E., and Timasheff, S. N. (1992) *Biochemistry* 31, 8080−8089.
16. Shearwin, K. E., Perez-Ramirez, B., and Timasheff, S. N. (1994) *Biochemistry* 33, 885−893.
17. Chrétien, D., Fuller, S. D., and Karsenti, E. (1995) *J. Cell Biol.* 129, 1311−1328.
18. Hyman, A. A., and Karsenti, E. (1996) *Cell,* 84, 401−410.
19. Saltarelli, D., and Pantaloni, D. (1982) *Biochemistry* 21, 2996−3006.
20. (a) Andreu, J. M., and Timasheff, S. N. (1982) *Proc. Natl. Acad. Sci. .U.S.A.* 79, 6753−67656. (b) Andreu, J. M., and Timasheff, S. N. (1982) *Biochemistry* 21, 6465−6476.
21. Andreu, J. M., Wagenknecht, T., and Timasheff, S. N. (1983) *Biochemistry* 22, 1556−1566.

22. Leynadier, D., Peyrot, V., Sarrazin, M., Briand, C., Andreu, J. M., Rener, G. A., and Temple, C., Jr. (1993) *Biochemistry* 32, 10675−10682.
23. De Ines, C., Leynadier, D., Barasoain, I., Peyrot, V., Garcia, P., Briand, C., Rener, G. A., and Temple, C., Jr.(1994) *Cancer Res.* 54, 75−84.
24. Barbier, P., Peyrot, V., Dumortier, C., D'Hoore A. Rener, G., and Engelborghs, Y. (1996) *Biochemistry* 35, 2008−2015.
25. Weisenberg, R. C., Borisy, G. G., and Taylor, E. (1968) *Biochemistry* 7, 4466−4479.
26. Lee, J. C., Frigon, R. P., and Timasheff, S. N. (1973) *J. Biol. Chem.* 248, 7253−7262.
27. (a) Fitzgerald, T. J. (1974) *Biochem. Pharmacol.* 25, 1383−1387. (b) Andreu, J. M., Gorbunoff, M. J., Lee, J. C., and Timasheff, S. N. (1984) *Biochemistry* 23, 1742−1752.
28. Temple, C., Jr., and Rener, G. A. (1989) *J. Med. Chem.* 32, 2089−2092.
29. Diaz, J. F., and Andreu, J. M. (1993) *Biochemistry* 32, 2747−2755.
30. Lakowicz, J. R. (1983) *Principles of Fluorescence Spectroscopy*, Plenum Press, New York.
31. Barbier, P., Peyrot, V., Sarrazin, M., Rener, G. A., and Briand, C. (1995) *Biochemistry* 34, 16821−16829.
32. Hummel, J. P. M., and Dreyer, W. J. (1962) *Biochim. Biophys. Acta* 63, 530−532.
33. Peyrot, V., Leynadier, D., Sarrazin, M., Briand, C., Menendez, M., Laynez, J., and Andreu, J. M. (1992) *Biochemistry* 31, 11125−1131.
34. Seckler, R., Wu, G. M., and Timasheff, S. N. (1990) *J. Biol. Chem.* 265, 7655−7661.
35. Andreu, J. M., and Timasheff, S. N. (1981) *Arch. Biochem. Biophys.* 211, 151−157.
36. Perez-Ramirez, B., Shearwin, K. E., & Timasheff, S. N. (1994) *Biochemistry* 33, 6253−6261.
37. Gilbert, L. M., and Gilbert, G. A. (1978) *Methods in Enzymology*, Volume XLVIII, Part F (Hirs, C. H. W., and Timasheff, S. N., Eds.) Academic Press, p 155, NY.
38. Ward, L. D., Seckler, R., and Timasheff, S. N. (1994) *Biochemistry* 33, 11900−11908.
39. Weisenberg, R. (1972) *Science* 177, 1104−1105.
40. Lee, J. C., and Timasheff, S. N. (1974) *Biochemistry* 13, 257−265.
41. Melki, R., and Carlier, M. F. (1993) *Biochemistry* 32, 3405−3413.
42. Allam, N., Millot, J. M., Leynadier, D., Peyrot, V., Briand, C., Temple, C., Jr., and Manfait, M. (1995) *Int. J. Biol. Macromol.* 17, 55−60.

BI970568T